STUDY OF A COMPLETE THERMOELECTRIC GENERATOR BEHAVIOR INCLUDING WATER-TO-AMBIENT HEAT DISSIPATION ON THE COLD SIDE

P. Aranguren, D. Astrain*, A. Martínez,

Department of Mechanical Engineering.

Public University of Navarre

Campus Arrosadia, Pamplona, 31006, Spain

***Tel: +34 948 169597, Fax: +34 948 169099, E-mail:** david.astrain@unavarra.es

Abstract

The reduction of the thermal resistances of the heat exchangers of a thermoelectric generation system (TEG), leads to a significant increase in the TEG efficiency. For the cold side of a thermoelectric module (TEM), a wide range of heat exchangers has been studied, form simple finned dissipators to more complex water (water-glycol) heat exchangers. As Nusselt numbers are much higher in water heat exchangers than in conventional air finned dissipators, convective thermal resistances are better. However, to conclude which heat exchanger leads to higher efficiencies, it is necessary to include the whole system involved in the heat dissipation, that is, TEM-to-water heat exchanger, water-to-ambient heat exchanger, as well as the required pumps and fans.

This paper presents a dynamic computational model able to simulate the complete behavior of a TEG, including both heat exchangers. The model uses the heat transfer and hydraulic equations to compute TEM-to-water and water-to-ambient thermal resistances, along with the resistance of the hot side heat exchanger at different operating conditions. Likewise, the model includes all the thermoelectric effect with temperature-dependent properties.

The model calculates the net power generation at different configurations, providing a methodology to design and optimize the heat exchange in order to maximize the net power generation for a whole variety of TEGs.

Keywords: thermoelectric generation; heat exchanger; heat dissipation; computational model.

Nomenclature

C_{p}	Specific heat	J/kgK
D_e	Pipe exterior diameter	m
D_i	Pipe interior diameter	m
f	Friction losses	
$h_e = \frac{Nu_{\mathrm{e}}k}{D_{\mathrm{e}}}$	Exterior convective coefficient	K/ m^{2}W
$h_i = \frac{Nu_{\mathrm{i}}k}{D_i}$	Interior convective coefficient	K/ m^{2}W
k	Thermal conductivity	W/mK
k_{local}	Local losses coefficient	
L	Pipe length	m
$\dot{m}$	Water mass flow	kg/s
Nu_{e}	Exterior Nusselt number	
Nu_{i}	Interior Nusselt number	
Pr	Prandtl number	
$\dot{Q}_{\mathrm{c}}$	Cold side heat power emission	W
$\dot{Q}_{\mathrm{f}}$	Water-to-ambient heat exchanger heat power exchanged	W
$\dot{Q}_h$	Heat flux transmitted to the TEM hot side	W
$\dot{Q}_{23}$	Heat power exchanged from TEM-to-water heat exchanger output to water-to-ambient heat exchanger input	W
$\dot{Q}_{41}$	Heat power exchanged from water-to-ambient heat exchanger output to TEM-to-water heat exchanger input	W
Ra	Raleigh number	
R_{c}	Cold side thermal resistance of the dissipation system	K/W
Re	Reynolds number	
R_{f}	Water-to-ambient heat exchanger thermal resistance	K/W
R_{h}	Hot side thermal resistance of the heat exchanger	K/W
R_{TEM}	TEM-to-water heat exchanger thermal resistance	K/W
T_{amb}	Ambient temperature	K
T_{H}	Heat source temperature	K

T_{TEM}	Cold side temperature	K
T_1	TEM-to-water heat exchanger input temperature	K
T_2	TEM-to-water heat exchanger output temperature	K
T_3	Water-to-ambient heat exchanger input temperature	K
T_4	Water-to-ambient heat exchanger output temperature	K
U_{e}	Exterior global heat transfer coefficient	K/Wm^2
U_{f}	Global heat transfer coefficient of the Water-to-ambient heat exchanger	K/ m^{2}W
U_{23}	Global heat transfer coefficient from TEM-to-water heat exchanger output to water-to-ambient heat exchanger input	K/ m^{2}W
U_{41}	Global heat transfer coefficient from water-to-ambient heat exchanger output to TEM-to-water heat exchanger input	K/ m^{2}W
v	Fluid velocity	m/s
$\dot{W}_{\mathrm{aux}}$	Electric power consumption of the auxiliary equipment	W
$\dot{W}_{\mathrm{fan}}$	Electric power consumption of the fan	W
$\dot{W}_{\mathrm{net}}$	Generated net electric power	W
$\dot{W}_{\mathrm{TEG}}$	Thermoelectric generated electric power	W
$\dot{W}_{\mathrm{pump}}$	Electric power consumption of the pump	W

Greek letters

$\varepsilon_{\mathrm{TEM}}$	TEM efficiency	
$\varepsilon_{\mathrm{total}}$	Total efficiency	
$\in$	Material roughness	m
ΔP_{tot}	Total hydraulic losses	kPa
ΔP_{TEM}	TEM-to-water heat exchanger hydraulic losses	kPa
ΔP_{ins}	Installation pipe hydraulic losses	
ΔP_{f}	Water-to-ambient heat exchanger hydraulic losses	kPa
ρ	Fluid density	kg/m^3

1. Introduction

One of the most important applications of thermoelectrics (TE) is the conversion of heat into electric power [1, 2]. In this field, TEGs present important advantages over other ways of providing

energy, such as turbines or thermal engines. TEGs have less maintenance and are more compact, robust and reliable since they are easily controlled and lack of moving parts. Due to their advantages, TEGs have had a key role in the aero spatial field. For more than 40 years TEGs have been producing electricity for various spacecraft, from Transit missions (1961-1964) to MSL-Curiosity (2011) [3, 4].

Nowadays, several researches work on waste heat recovery applications, that is waste heat turned into electricity. The amount of waste energy being thrown away to the atmosphere is enormous and TEGs are a good option because of the positive facts mentioned before. In this sense a possible application stays in the automotive sector, and intends to generate electric power form the heat wasted though the tailpipes. This technology produces a reduction of approximately 5% in the fuel consumption [5, 6]. Likewise, heat recovery in the industrial sector, both in the manufacturing sector and in the electric generation industries, is also a very interesting application [7]. A theoretical study showed that 100MW electric power could be recovered by TEG installed in all the cogeneration plant in Thailand.

Efforts are devoted to increase the efficiency of the TEM. Most researchers focus on improving the figure of merit [9, 10] of thermoelectric materials whereas some intend to improve the efficiency of TEGs by optimizing the heat exchangers on the hot and cold side of the TEM. These devices transfer heat form the heat source to the hot side of the TEM and from the TEM cold side to the ambient, respectively. The importance of reducing the thermal resistances of these heat exchangers to maximize the efficiency has been already revealed [1].

Numerous studies focus on optimizing the thermal resistance of the heat exchanger on the cold side [2, 11, 12], were heat exchangers with water as working fluid emerge as a promising alternative. Heat exchangers with refrigerant fluids have higher convective coefficients than common finned dissipators with or without fans [13]. Last researches focus on water heat exchanger optimization, were the number of channels or the cross areas are studied to obtain the highest convective coefficients [14]. It has also been demonstrated that microgeometry on water heat exchangers leads to similar generated power with lower water mass flow [15].

Those works indicate high thermal resistances for water heat exchangers located on the cold side of the TEM. However, those studies are not complete, since to compute the real thermal resistance on TEM cold side, it is necessary to include also the thermal resistance of the water-to-ambient heat

exchanger. The water temperature increases due to the heat absorbed from the TEMs, so a second heat exchanger is needed to cool down the water, exchanging heat with the ambient. A dissipation system for the cold side includes the TEM-to-water heat exchanger, a pump to make water circulate along the pipes, a water-to-ambient heat exchanger and connecting pipes. Every component should be accounted for to get the final thermal resistance and the auxiliary power consumption.

This paper presents a calculation methodology based on a computational model which obtains the total thermal resistance, as well as the auxiliary equipment power consumption (the pump and the fans). The total thermal resistance is composed by that of the TEM-to-water heat exchanger, the water-to-ambient heat exchangers and the connecting pipe. This model combines with a previous computational model [1] that calculates the generated electric power and the efficiency of the TEGs to finally provide net generated power. This methodology is used to optimize this net power. Different configurations for the TEM cold side dissipation system are studied; both the conventional finned dissipators and the water heat exchanger technology are contemplated.

2. Objectives

The main objective of this paper is to conduct a computational study about the influence of the TEM cold side heat exchanger on the total efficiency of the TE system. Some specific objectives are stated:

- Implementation of a predictive computational model to simulate the whole behavior of a water dissipation system, including every element: TEM-to-water heat exchanger, water-to-ambient heat exchanger, pipes and a pump. This model will provide the power consumptions and the total thermal resistance.
- Water heat exchanger and finned dissipator comparative study.
- Interaction of the developed computational model with the previous one [1] to obtain the generated net power of a TEG.
- Comparative study of five different configurations of the cold side heat exchanger to maximize the generated power and efficiency of the TEG.

3. Methodology and computational model

A TEG is composed of three parts: TE module(s), a hot side heat exchanger, which exchanges heat

from the heat source to the TEM hot side, and the cold side heat exchanger.

The simplest cold side heat exchanger is a finned dissipator with a fan as Fig.1a) shows. However, there exists an alternative that uses using a liquid as a working fluid (normally water or water mixed with an alcohol). This liquid transports the heat from the TEM to the ambient. This configuration has been lately studied [2, 13, 14] owning to the high cooling potential offered by the fluid. This system is more complex because of the additional elements that can be seen in Fig. 1b:

1. TEM-to-water heat exchanger. It is a plate with channels where the liquid circulates through to absorb the heat coming from the TEM
2. Connecting pipes. Some pipes connected to the different elements and a pump to make the liquid circulate.
3. Water-to-ambient heat exchanger. Its principal goal is to dissipate heat from the liquid to the ambient. This heat exchanger can have a fan to create forced convection or simply work by natural convection.

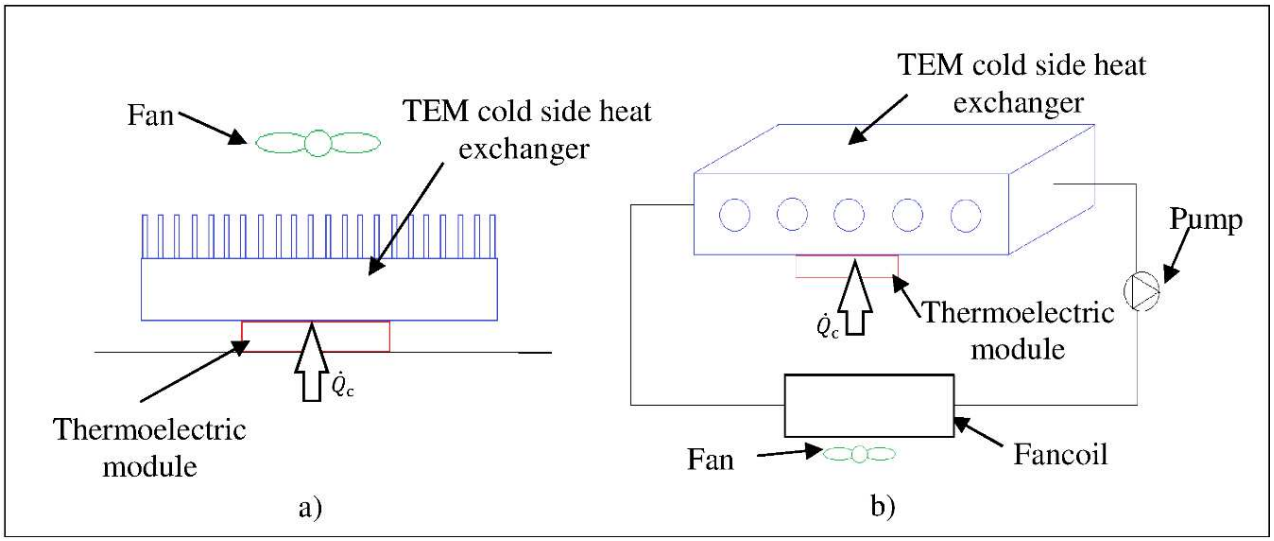

Fig. 1 a) Finned dissipator, b) Heat exchanger with a refrigerant fluid

3.1. Methodology

To design and optimize a TEG for a specific application, it is necessary to obtain two main parameters: the TE generated power which depends on the temperature of the TEM sides, and the electric power consumption of the auxiliary equipment. The temperature of the TEM is set by the heat

exchangers situated on both sides. The generated net power consumption is maximized throughout Equation (1).

$$\dot{W}_{\text{net}} = \dot{W}_{\text{TEG}} - \dot{W}_{\text{aux}} \quad (1)$$

Where:

$$\dot{W}_{\text{aux}} = \dot{W}_{\text{pump}} + \dot{W}_{\text{fan}} \quad (2)$$

In [1] the TE generation predictive model was presented. Its accuracy was higher than the 95%. The generated power was provided as a function of the heat exchanger thermal resistances.

$$\dot{W}_{\text{TEG}} = f(R_{\text{h}}, R_{\text{c}}) \quad (3)$$

In the present paper, another computational model has been implemented to calculate the total thermal resistance cold side heat exchanger, as well as the power consumptions of the auxiliary equipment. It requires as input parameter the heat emitted by the TEM cold side, which has to be dissipated by the system, as Equations (4) and (5) indicate.

$$\dot{Q}_{\text{c}} = \dot{W}_{\text{TEG}} \left(\frac{1}{\varepsilon_{\text{TEM}}} - 1 \right) \quad (4)$$

$$\varepsilon_{TEM} = \frac{\dot{W}_{\text{TEG}}}{\dot{Q}_{\text{h}}} \quad (5)$$

To calculate the heat dissipated, it is necessary to know the TE generated power, as well as the TEM efficiency. These values depend on the thermal resistances of both heat exchangers. In turn, these resistances depend on the heat dissipated. Therefore, an iterative method between the two computational models is proposed. Fig. 2 shows the steps followed to finally get the net generated power.

In this methodology, the thermal resistance on the TEM hot side (R_{h}) is not included in the iterative calculation. This is because it is a heat exchanger which does not present auxiliary equipment. It is important to note that the methodology would also be applicable in case this heat exchanger had auxiliary equipment.

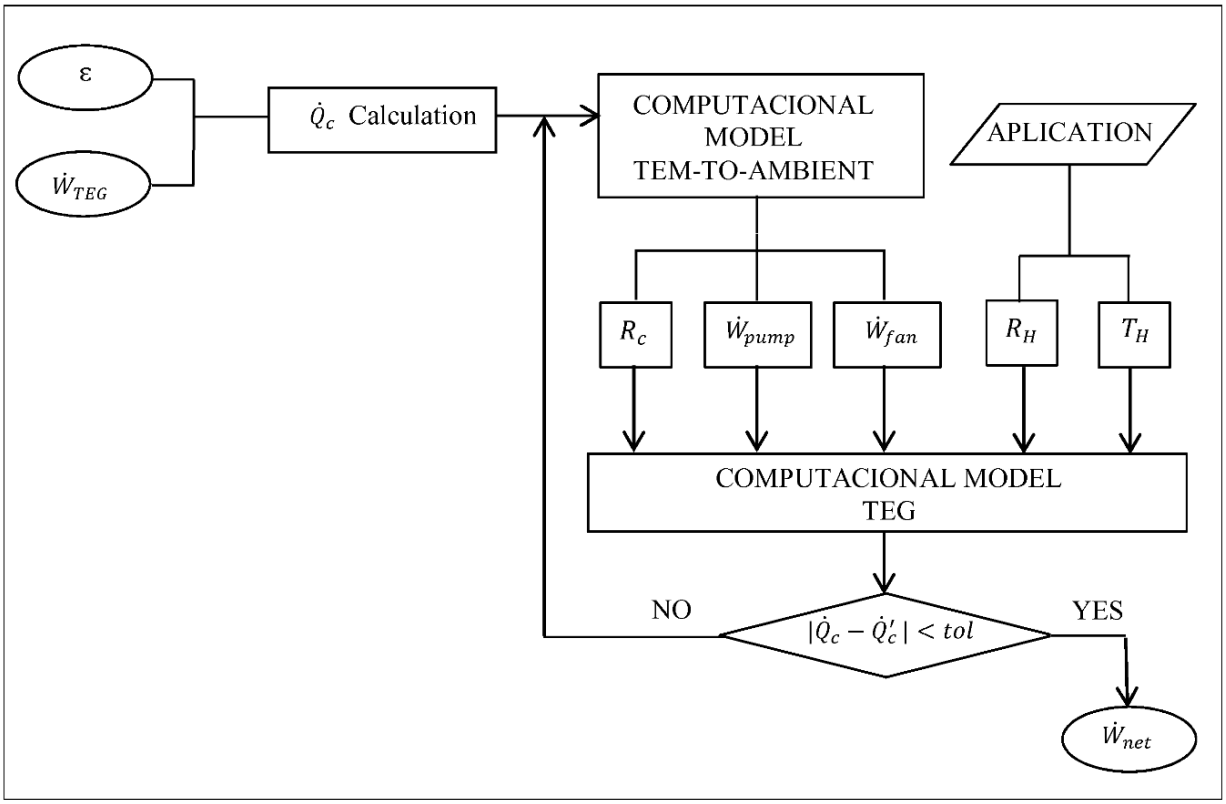

Fig. 2 Methodology of the interaction between computational models.

3.2. TEM-to-ambient heat exchanger computational model

The computational model solves the thermal and hydraulic expressions and follows the methodology shown in Fig. 3. It computes pressure losses and thermal resistances as a function of the air and water mass flows for every element of the dissipation system.

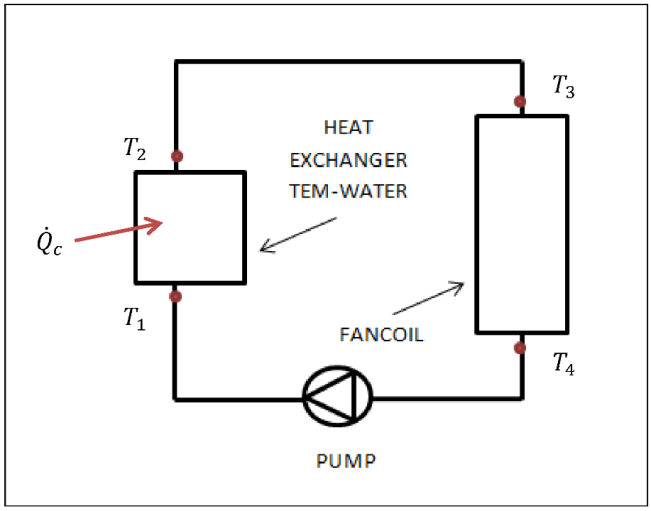

Fig. 3 Schematic of total thermal resistance calculation computational model.

This model solves thermal and hydraulic expressions for a range of water mass flows. Once

every point of the range is solved, the characteristic curve of the hydraulic system is achieved. The intersection of this curve with the pump curve provides the operating point.

3.2.1. Thermal calculation

Equation (6) shows the total thermal resistance of the system. R_c which is formed by that of the TEM-to-water heat exchanger, water-to-ambient heat exchanger and connecting pipes.

$$R_c = \frac{T_{TEM} - T_{amb}}{\dot{Q}_c} \tag{6}$$

The heat flux coming from the TEM cold side ($\dot{Q}_c$), which corresponds to the heat dissipated into the ambient through the elements of the system, must be calculated to obtain Equation (6). Four are the temperatures to find, the input and output of both heat exchangers, as it can be seen in Fig. 4. Given $\dot{Q}_c$ the temperature difference $\Delta T_{12} = (T_2 - T_1)$ is known through Equation (7):

$$\Delta T_{12} = \frac{\dot{Q}_c}{C_p \cdot \dot{m}} \tag{7}$$

The method used is an iterative process since the four temperatures and the heat fluxes are unknown. The starting point is the assumption of three temperatures: T_1, T_3 and T_4. Utilizing Equation (7), T_2 is obtained, so the four temperatures are set for further calculation. The heat transfer global coefficients are calculated throughout Equation (8) [16]:

$$U_e = \frac{1}{\frac{D_e}{D_i h_i} + \frac{\frac{D_e}{2}\ln\left(\frac{D_e}{D_i}\right)}{k} + \frac{1}{h_e}} \tag{8}$$

The heat transfer coefficient includes the internal convection, conduction and external convection. The expressions for laminar and turbulent flow are given by Equations (9) - (11).

Internal convection:

$$Nu_i = 0.023 Re_D^{0.8} \mathrm{Pr}^{0.3} \quad Re > 2300 \tag{9}$$

$$Nu_i = 3.66 + \frac{0.0668\left(\frac{D}{L}\right) Re_D \mathrm{Pr}}{1 + 0.04\left(\left(\frac{D}{L}\right) Re_D \mathrm{Pr}\right)^{2/3}} \quad Re < 2300 \tag{10}$$

$$Nu_i = 3.66 \quad Re < 2300 \; and \; Developed \; region \tag{11}$$

For the external convective coefficient, two different scenarios have been studied, natural convection and forced convection provided by a fan.

$$Nu_{\mathrm{e}} = \left(0.6 + \frac{0.387 Ra_{\mathrm{D}}^{1}}{\left(1 + \left(\frac{0.559}{\mathrm{Pr}}\right)^{\frac{9}{16}}\right)^{\frac{8}{27}}} \right)^{2} \quad Natural\ convection \tag{12}$$

$$Nu_{\mathrm{e}} = 0.3 + \frac{0.62 Re_{D}^{\frac{1}{2}} \mathrm{Pr}^{\frac{1}{3}}}{\left(1 + \left(\frac{0.4}{\mathrm{Pr}}\right)^{\frac{2}{3}}\right)^{\frac{1}{4}}} \left(1 + \left(\frac{Re_{D}}{28200}\right)^{\frac{5}{8}}\right)^{\frac{4}{5}} \quad Forced\ convection \tag{13}$$

In the water-to-ambient heat exchanger (a fancoil) the calculation of the heat transfer coefficient needs different expressions due to its geometry. This heat exchanger exhibits of a core composed of pipes and transversal fins. A fan is included to force the air flow through the fins. In this case, efficiency expressions are needed to characterize the heat transfer. Heat transfer coefficients and temperatures provide the heat fluxes transferred from the different elements to the ambient as Equations (14) – (16) indicate.

$$\dot{Q}_{\mathrm{f}} = \frac{U_{\mathrm{f}} A_{\mathrm{f}} \left((T_3 - T_{\mathrm{amb}}) - (T_4 - T_{\mathrm{amb}}) \right)}{\ln\left(\frac{(T_3 - T_{\mathrm{amb}})}{(T_4 - T_{\mathrm{amb}})} \right)} \tag{14}$$

$$\dot{Q}_{23} = \frac{U_{23} A_{23} \left((T_2 - T_{\mathrm{amb}}) - (T_3 - T_{\mathrm{amb}}) \right)}{\ln\left(\frac{(T_2 - T_{\mathrm{amb}})}{(T_3 - T_{\mathrm{amb}})} \right)} \tag{15}$$

$$\dot{Q}_{41} = \frac{U_{41} A_{41} \left((T_4 - T_{\mathrm{amb}}) - (T_1 - T_{\mathrm{amb}}) \right)}{\ln\left(\frac{(T_4 - T_{\mathrm{amb}})}{(T_1 - T_{\mathrm{amb}})} \right)} \tag{16}$$

Therefore, once these expressions are solved and Equation (17) is applied to every element, a linear equation system is achieved, composed of three equations with three unknowns, that finally provides T_1, T_3 and T_4.

$$\dot{Q}_{ij} = \dot{m} C_{\mathrm{p}} \Delta T_{\mathrm{ij}} \tag{17}$$

This process is repeated until the temperature difference between two consecutive iterations drops below an established value.

3.2.2. Hydraulic calculation

Total hydraulic losses are formed by the addition of different pressure losses along each element

of the system, as Equation (18) indicates.

$$\Delta P_{\mathrm{tot}} = \Delta P_{\mathrm{TEM}} + \Delta P_{\mathrm{ins}} + \Delta P_{\mathrm{f}} \tag{18}$$

Pressure losses are divided into primary and secondary whose characteristic coefficients are $\frac{fL}{D}$ and k_{local}, respectively [15]:

$$\Delta P = \frac{v^2}{2}\left(\frac{fL}{D} + k_{\mathrm{local}}\right) \cdot \frac{\rho}{1000} \tag{19}$$

Friction coefficient, (f), is a function of the fluid flow inside the pipes. Reynolds number determines if the fluid flow is laminar or turbulent, so as to apply Equation (20) or Equation (21), respectively [17].

$$f = \frac{64}{Re_{\mathrm{D}}} \quad Re < 2300 \tag{20}$$

$$f = \frac{1}{\left(-1.8 \cdot \log\left(\left(\frac{6.9}{Re_{\mathrm{D}}}\right) + \left(\frac{\in}{3.7D_{\mathrm{i}}}\right)^{1.11}\right)\right)^2} \quad Re > 2300 \tag{21}$$

Fluid properties depend on temperature, so velocity and temperature should be known to calculate the hydraulic losses along the different elements of the system. That is the reason why the thermal calculations have been done before. Knowing the mass flow, velocities can be calculated throughout the cross area of the pipes. However, the TEM-to-water heat exchanger has parallel channels, so the mass flow along each channel is unknown. Due to the local losses at channel inputs and outputs, it cannot be considered that every channel has the same mass flow. Noticing that the friction coefficient depends on mass flow, it is necessary to solve a nonlinear system. The procedure to solve hydraulic losses in the TEM-to-water heat exchanger is also an iterative method.

Secondary loss coefficients are only dependent on the pipe geometry and setting up. Some specific values used are: $k_{elbow} = 0.5,\ k_{entry} = 0.5,\ k_{exit} = 1, k_{branchflow} = 1,\ k_{lineflow} = 0.25$ [17].

The resolution of the thermal and hydraulic expressions for every mass flow provides the system characteristic curves. The intersection of the pump curve and the hydraulic losses curve provides the operating point, that is, the mass flow that is circulating along the system. This information provides the thermal resistances of the system. Since the goal of the model is to obtain the total thermal resistance of the dissipation system, TEM temperature has to be known. Equation (22) calculates TEM temperature throughout TEM-to-water heat exchanger thermal resistance. The resolution of this resistance is more

complicated than utilizing the expressions seen before. This resistance is formed by the addition of the conductive resistance, calculated through a computational fluid dynamics (CFD) software, Fluent, the contact resistance, experimentally obtained, and the internal convection resistance provided by Nusselt expressions.

$$\dot{Q}_{\mathrm{c}} = \frac{\left(T_{\mathrm{TEM}} - \frac{T_1 + T_2}{2}\right)}{R_{\mathrm{TEM}}} \tag{22}$$

Fig. 4 shows the computational model flowchart.

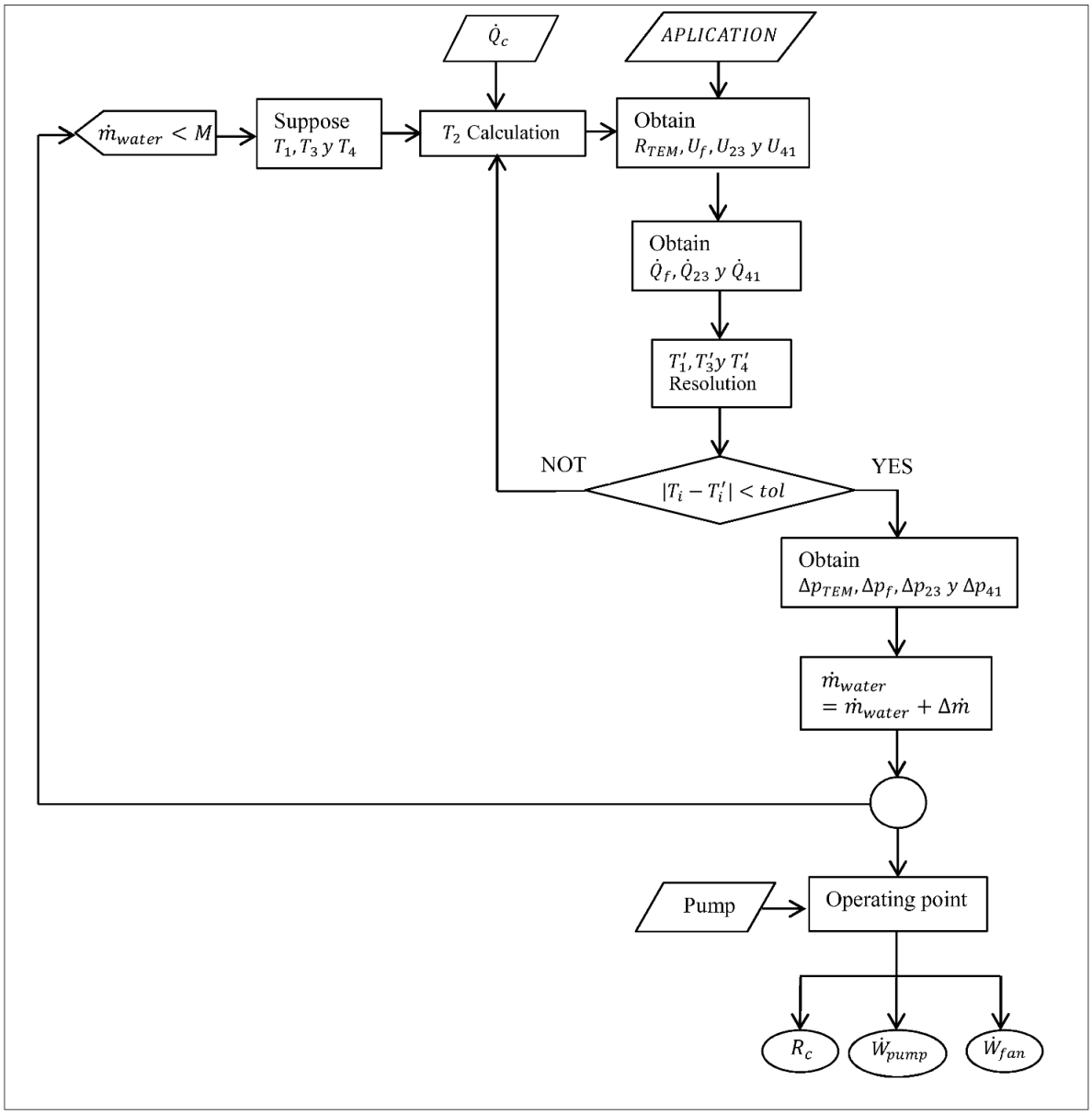

Fig. 4 Flowchart of the cold side heat exchanger calculation computational model.

3.2.3. CFD Verification

The objective of this section is to assess whether or not the values obtained with the computational model are in a good agreement with the values achieved by the CFD software, Ansys Fluent. This verification focuses on the TEM-to-water heat exchanger. The simulation of the whole dissipation system (the two heat exchangers, the pump and the pipes) with CFD would require a huge amount of time as well as a really powerful computer. Furthermore, the results obtained from the CFD program would represent just a specific geometry, and a whole new simulation (geometry, meshing and fluid calculations) would be required for a new geometry. However, the computational model developed in this paper is suitable for the simulation of any thermal resistance. This fact makes this methodology so powerful for calculation and design of TEGs.

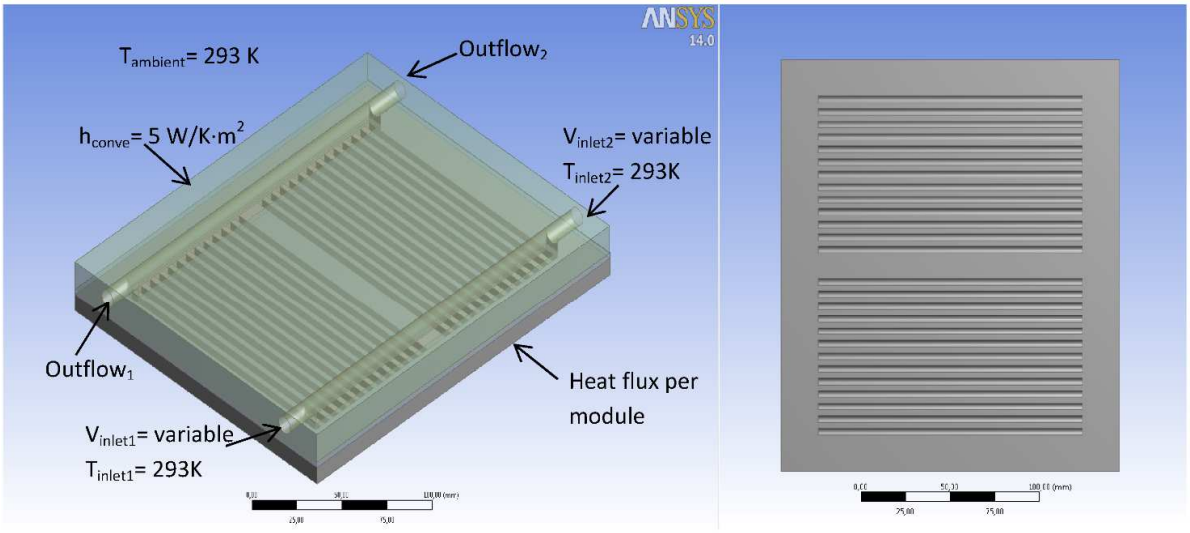

Fig. 5 Geometry description of the TEM-to-water heat exchanger, a) Dissipator external geometry and boundary conditions, b) Channels middle plane.

The particular heat exchanger that has been simulated includes 4 mm diameter channels and two inputs and two outputs. This heat exchanger dissipates heat from 12 TEM. The mesh of this geometry is crucial, since it has to be small enough to predict the thermal effects inside the channels, but big enough to reach the solution in a reasonable period of time. Collector and channels distribution can be seeing in Fig. 5 a). Fig. 5 b) shows a detail of the mesh.

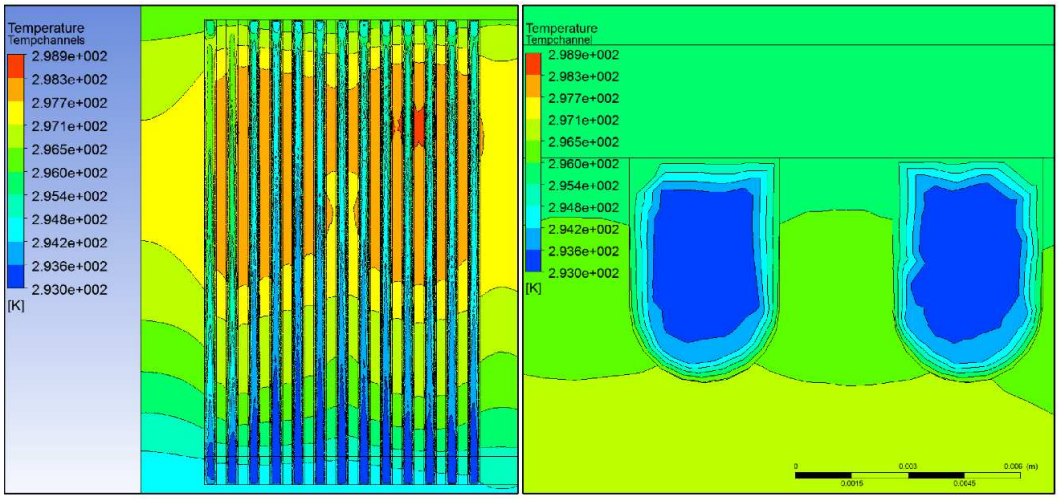

a) b)

Fig. 6 Thermal behavior of the TEM-to-water heat exchanger, a) Distribution of the temperature in the channels middle plane, b) Water temperature distribution at the channels cross area.

Fig. 6 represents the thermal distribution. Fig. 6 a) shows the water as it flows along the channels. The symmetry of the thermal contours implies that the simulation has reached a stationary point, so the desired solution has been found. Fig. 6 b) shows the importance of creating a small mesh to account for wall effects in the channels. Fig. 7 shows the thermal resistance versus the water mass flow provided by both the CFD software and computational model. As can be seen, the computational model predicts the heat exchanger behavior accurately and properly computes the dependence of the thermal resistance with the mass flow. The maximum deviation in the thermal resistance is 5%. Furthermore, the computational time decreases a 99.9% compared to that required by the CFD program.

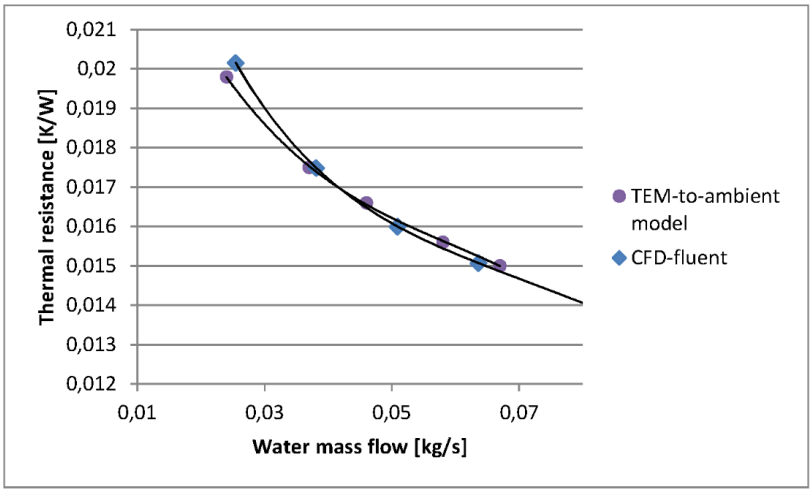

Figure. 7 CFD and computational model thermal resistances comparison.

Thus, the computed thermal resistance values are proven to be consistent, giving credibility to the results in Section 5.

4. Studied cases

Given the great potential that thermoelectric technology has for waste heat recovery [5-7], this work uses as heat source the heat of the smokes of a combustion process. Specifically, the smokes come from the combustion boiler of a paper mill located in Sangüesa (Navarra), Spain.

The characteristics of the smoke are provided by Table I data. The smoke temperature at the chimney is 200ºC while the mean ambient temperature of the location is 15ºC [1].

Heat source (Combustion smoke)	
$\dot{m}_{\text{smoke}}$	20.9 kg/s
v_{smoke}	21.52 m/s
A_{smoke}	0.88 x 0.88 m^2
$C_{\text{p,smoke}}$	1087.8 J/kgK
ρ_{smoke}	1.254 kg/m^3
T_{smoke}	473 K

Table I Smoke characteristics.

The TEG system is composed of 144 Marlow TG 12-8-01L TEM specially fabricated for generation that occupy an area of 0.33 m^2. Operating temperatures can be as high as 250ºC [18], since their welds are special to endure high operating temperatures. Module dimensions are 40x40 mm^2 and its thickness is 3.53 mm. It encloses 127 thermocouples fabricated in bismuth and tellurium. Total TEG occupied area ratio is $\frac{A_p}{A_b} = 0.7$, that is, the 70% of the total area is occupied by the TEM.

The TEG system is directly located on the chimney. A finned dissipator is located on the TEM hot side. This heat exchanger has a thickness of 10 mm, 35mm length fins with a thickness of 2mm and a fin spacing of 10mm. Due to the high occupation ratio, the thermal resistance of the hot side heat exchanger is 1.63K/W, as was demonstrated in [1].

The cases studied have various cold side heat exchangers:

4.1. Case 1. Finned dissipator and fan

The aluminum finned dissipator has a thickness of 14mm and a fin length of 25 mm. The thickness and spacing of the fins are 1.5 and 2.46 mm respectively. Over the dissipator, a fan is situated

to make air circulate over the fins, increasing the convective coefficient. The cold side thermal resistance is 0.44K/W.

The operating point and power consumption of the fan have been obtained through the air losses and the necessary air mass flow to get the resistance mentioned. The 5.5 W fan SUNON MEC02551V1-0000-A99 has been used to extrapolate the power consumption, obtaining a total power consumption of 60W.

4.2. Case 2. TEM-to-water heat exchanger and fancoil-1

The TEG is located at a 2m height. The 144 TEM form 4 parallel branches, each one composed by 36 TEM. The total water flow, that is, the sum of the water that circulates along every branch, is cooled down at a unique fancoil. A WILO-Stratos PICO 15/1-6-130 pump is the responsible for making the water circulate. The power consumption of the pump is 40 W with a maximum head of 6 meters.

The fancoil is composed of 24 tubes, 0.6 meters long, with a total cross area of 0.12 m^2. The tubes are embedded in a finned kernel while some fans move the air into the fin spacing to achieve higher convective coefficients. The thickness of the fins is 0.2mm and its spacing is 1.6mm. The fancoil geometry provides compactness to the TEG. Furthermore, 30W of extra power consumption is needed to procure a thermal resistance of 0.48 K/W. This value has been obtained with the computational model explained along Section 3.2.

4.3. Case 3. TEM-to-water heat exchanger and fancoil-2

The TEM configuration is the same as that in Case 2. The difference is the fancoil size. Now, the total facoil length is 1.2 m with a total heat transfer area of 0.25 m^2; the area has been doubled from Case 2. The total fan consumption is 60W to achieve a thermal resistance of 0.38 K/W.

4.4. Case 4. TEM-to-water heat exchanger and natural convection

This one is similar to Case 2, but it doesn't include a fan, so natural convection occurs over the fins. In this case, the only consuming power is the one required by the pump. The total heat transfer area has been significantly increased up to 0.96 m^2. The thermal resistance obtained is 0.42 K/W

4.5. Case 5. TEM-to-water heat exchanger and 0.5 m/s wind velocity

This configuration is similar to that in Case 4, but with a small wind velocity (0.5 m/s) that increases the convective coefficient and improves the thermal resistance.

5. **Results**

The results have been obtained through the interaction of the two computational models showed in Fig. 2. Case 1 has not needed the interaction between models because the heat exchanger was a simple finned dissipator. In this case, just the TEG computational model was used. The objective of this study is to compare the efficiency of the TEG, provided by Equation (23), among the different heat dissipation systems.

$$\varepsilon_{\text{total}} = \frac{\dot{W}_{\text{net}}}{\dot{Q}_{\text{h}}} \tag{23}$$

The operating point of each dissipation system is crucial, since the thermal resistances highly depend on the water mass flow, which at the same time depends on the pump and the connecting pipes. Fig. 8 and Fig. 9 show the dependence of the thermal resistances on the water mass flow. Figure 10 provides the comparison between natural convection and forced convection with 0.5 m/s of wind velocity.

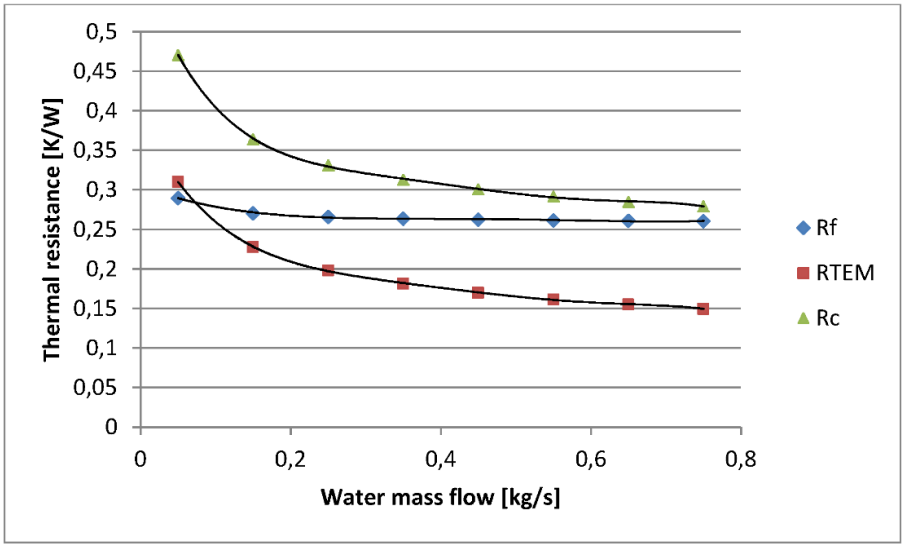

Fig. 8 Case 3 main thermal resistances.

Fig. 8 and 9 show the strong dependency of the total thermal resistance, R_c, with the water mass flow. However the main two thermal resistances that form the total thermal resistance have different behaviors. R_{TEM} has strong dependency on water mass flow whereas the dependence of R_{f} with the flow is negligible. The latter happens because at the fancoil, the dominant convection coefficient is the external one, which highly depends on the air mass flow but not on the water mass flow. As a

consequence, the water mass flow has negligible influence on the fancoil performance. On the other hand, at the TEM-to-water heat exchanger, the governing heat transfer mechanism is the internal convection, completely dependent on the water mass flow.

Fig. 8 indicates that the increasing of the water mass flow, by increasing the pump consumption, does not entail a significant decrease of total thermal resistance. This is because the total thermal resistance is limited by the fancoil thermal resistance, which presents no dependency on water mass flow, as previously indicated.

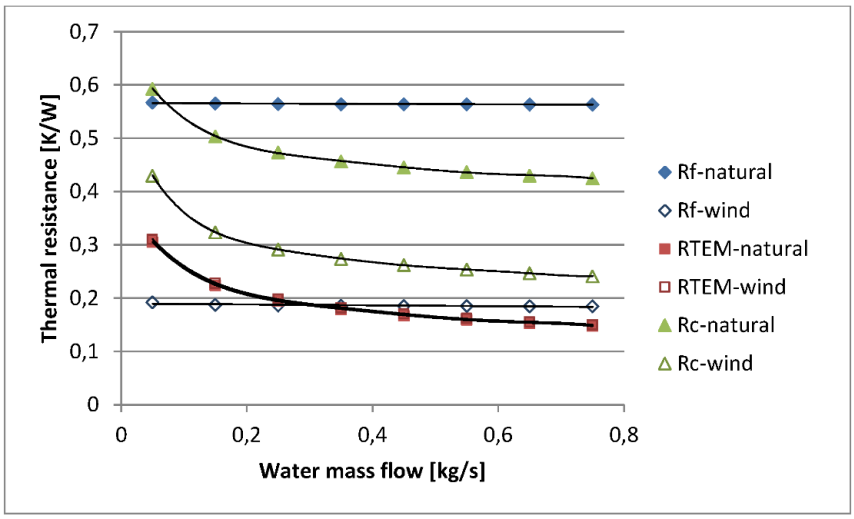

Figure. 9 Case 4 and Case 5 main thermal resistances.

Fig. 9 underlines the importance of accounting for the thermal resistances of the connecting pipes. When natural convection occurs, the fancoil thermal resistance is higher than the total thermal resistance, which can only be explained by the fact that part of the heat emitted by the TEM cold side is transferred into the ambient through the pipes. Piping composition and air velocity are the decisive factors in piping thermal resistances.

	R_c $[K/W]$	R_{TEM} $[K/W]$	R_f $[K/W]$	$\dot{W}_{TEM}$ $[W]$	$\dot{W}_{pump}$ $[W]$	$\dot{W}_{fancoil}$ $[W]$	$\dot{W}_{net}$ $[W]$	$\dot{Q}_c$ $[W]$	ε_{TEM}	ε_{total}
Case 1	0.44	--	--	221	0	60	161	53.78	2.78	2.02
Case 2	0.48	0.22	0.53	215	40	30	145	53.16	2.73	1.84
Case 3	0.38	0.24	0.27	231	40	60	131	54.7	2.85	1.61
Case 4	0.57	0.28	0.56	201	40	0	161	51.87	2.62	2.09
Case 5	0.42	0.28	0.19	224	40	0	184	54.1	2.80	2.3

Table II Every studied case output parameters.

Air velocity is determinant for the total thermal resistance in absence of fans. A small wind velocity of 0.5 m/s can lead to a 25% reduction in the thermal resistance.

Table II summarizes the computational results obtained for the five cases. It presents the total thermal resistance, TEM-to-water heat exchanger thermal resistance, water-to-ambient thermal resistance, auxiliary equipment consumptions, TE generated power, heat dissipation and TEM and total efficiencies. Fig. 10 presents power consumptions and electric power generation for every case, and the total thermal resistance.

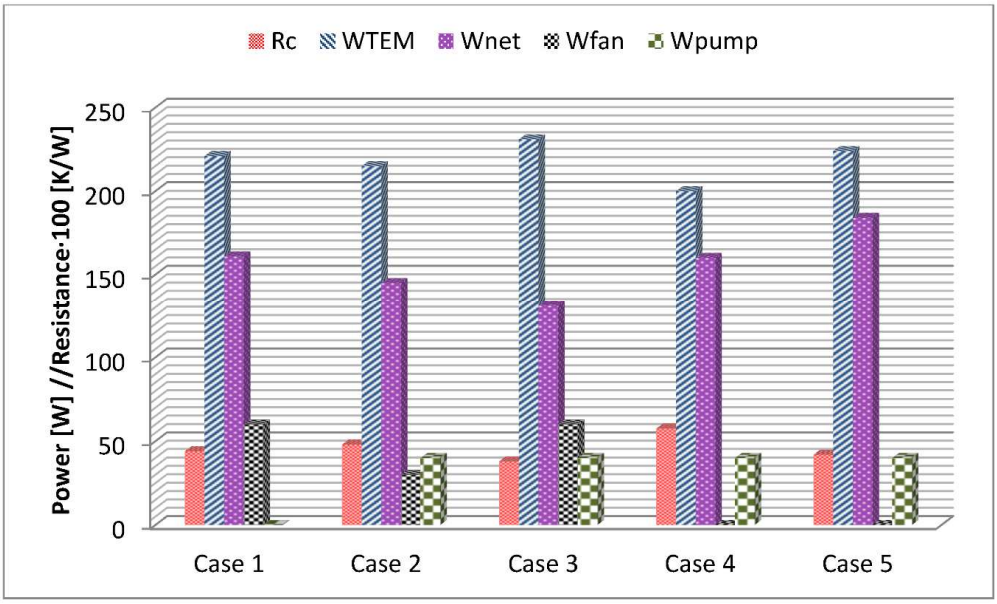

Figure. 10 Consumption and power generation of the studied cases.

From a thermal point of view, the best case is Case 3, since it has the smallest thermal resistance. However, it exhibits worst total efficiency, due to the consumption of the auxiliary equipment, which is higher than that in any other case and causes the drop of the net generated power.

TEM-to-water thermal resistance is smaller than the thermal resistance of Case 1, where only a fin dissipator is installed. However, the generated power is smaller in Case 2 where the heat exchanger with water as working fluid is simulated. This situation shows that TEM-to-water dissipator is not the only heat exchanger that should be accounted for when designing dissipation systems. In case 2, the fancoil resistance makes the total thermal resistance grow up to a higher value than that in Case 1, so the electric power generation is lower. Not only this event happens, but also the consumption of the auxiliary equipment grows, reducing even more the net power.

Cases 4 and 5 have no fans, so the auxiliary consumption only includes the pump. As the auxiliary consumption decreases, even with higher thermal resistances, the net power are higher than those obtained in the rest of the cases.

6. **Conclusions**

A computational model has been implemented for the TEM-to-ambient heat dissipation system. This computational model simulates the TEM-to water heat exchanger and the subsequent afterwards water cooling. The water cooling circuit includes a pump, a water-to-ambient heat exchanger and the connecting pipes. This model calculates the total thermal resistance of the dissipation system, electric power consumption, as well as, the influence of water and air mass flows.

The interaction of the two computational models creates a powerful calculation and design methodology for TEG, capable of predicting the TE net power generation. As was stated, auxiliary consumption must be taken into account when maximizing net generation power.

Throughout the study of five different cases, it has been proved that studying the TEM-to-water thermal resistance alone is not enough. It can happen that, despite this resistance is lower than the thermal resistance of a finned dissipator, the total resistance of the water dissipation system could be higher than that of the dissipator. This issue can happen because of the fancoil thermal resistance.

Another important conclusion is the fact that the case with the best thermal resistance is not the case with highest net power generation. The increase in the power consumption of the auxiliary equipment is higher than the increase in the TE power generation that entails the decrease in the TEM cold side thermal resistance. Thus, this methodology is capable of optimizing the dissipation system as a whole, taking into account thermal resistances and power consumptions.

Among the studied cases, Case 3 has the smallest thermal resistance, so the TE power generated is the highest one. However, it has the lowest net power, owning to the auxiliary equipment consumption. Case 4 and Case 5, which have no fans, have the best net power generation, but require bigger heat exchange areas.

Acknowledgments

The authors are indebted to the Spanish Ministry of Economy and Competitiveness, and European Regional Development Fund for the economic support to this work, included in the DPI2011-24287 research project.

References

[1] D. Astrain, JG. Vián, A.Martínez, A. Rodríguez, Energy 35, 602 (2010)

[2] C. Baker, P. Vuppuluri, L. Shi, M. Hall, J. Electron. Mater. 41,1290 (2012)

[3] D.M. Rowe, Thermoelectrics Handbook Macro to Nano, 1st edn. (CRC Press, Boca Raton, FL, 2006)

[4] V.P. Friedensen, Acta Astronautica 42, 395 (1998)

[5] J. LaGrandeur, D. Crane, S. Hung, B. Mazar, A. Eder, Proceedings of the XXV International conference on Thermoelectrics 343 (2006).

[6] C. Yu, K.T. Chau, Energ. Convers. Manage. 50, 1206 (2009)

[7] L.E. Bell, Science 321, 42 (2008)

[8] P. Yodovard, J. Khedari, J. Hirunlabh, Energ. Source. 23, 213 (2001)

[9] S. Wang, G. Tan, W. Xie, G. Zheng, H. Li, J. Yang, X. Tang, J. Mater. Chem. 22, 20943 (2012)

[10] D. Parker, D.J., Singh, Phys. Rev. 1, 1 (2011)

[11] Y. Zhou, J. Yu. Int. J. Refrig. 35, 1139 (2012)

[12] X. Gou, H. Xiao, S. Yang. Appl. Energ. 87, 3131 (2010)

[13] Z.G. Zhou, D.S. Zhu, H.X. Wu, H.S. Zhang, J. Therm. Sci. 22, 48 (2013)

[14] D. T. Crane, G.S. Jackson, Energ. Convers. Manage. 45, 1565 (2004)

[15] A. Rezania, L.A. Rosendahl, J. Electron. Mater. 45, 481 (2011)

[16]F.P. Incropera, D.P. Dewitt, T.L. Bergmann, A.S. Lavine, Fundamentals of Heat and Mass Transfer, 6th edn., p. 401, p.485, p.559.

[17] F. M. White, Fluid Mechanics, 6th edn., pp .382-393

[18] Marlow thermoelectric modules. http://www.marlow.com/products/power-generators/standard-generators/tg12-8-01l.html. Accessed December 2013.